

# Theoretical Study for Deformation Kinetics of Glassy Solid Helium within Cylindrical Microtubes

Zotin K.-H. Chu

*3/F, 4, Alley 2, Road Xiushan, Leshanxinchun, Xujiahui 200030*

## Abstract

We study the deformation kinetics for the (glassy) solid helium confined in microscopic domain at very low temperature regime by using an absolute-reaction-rate model considering the shear thinning behavior which means, once material being subjected to high shear rates, the viscosity diminishes with increasing shear rate. Our calculations show that there might be nearly frictionless fields for rate of deformation due to the almost vanishing shear stress in microtubes at very low temperature regime together with wavy-rough corrugations along micropores and the slip. As the tube size decreases, the surface-to-volume ratio increases and therefore, surface roughness will greatly affect the deformation kinetics in micropores. After using the boundary perturbation method, we have obtained a class of temperature and activation energy dependent fields for the deformation kinetics at low temperature regime with the presumed small wavy roughness distributed along the wall of an cylindrical microtube. The critical deformation kinetics of the glassy matter is dependent upon the temperature, activation energy, activation volume, orientation dependent and is proportional to the (referenced) shear rate, the slip length, the amplitude and the orientation of the wavy-roughness. Finally, we also discuss the quantitative similarity between our results with Ray and Hallock [Phys. Rev. Lett. **100**, 235301 (2008)].

PACS numbers: 67.80.K-, 67.80.B-, 67.25.dr, 83.60.St, 83.60.Rs, 83.50.Lh

## I. INTRODUCTION

Grigor'ev *et al.* recently performed high-precision pressure measurement in solid  $^4\text{He}$  samples grown by capillary blocking technique. In all their nonannealed hcp crystals, the temperature dependence of pressure demonstrates a contribution proportional to  $T^2$ , the latter becomes the leading term at temperatures  $T < 300$  mK, at which *supersolid* effects were observed. Grigor'ev *et al.* thus claimed that such a behavior may be ascribed to a glassy phase. They also found that this glassy contribution to pressure can be eliminated only by a substantial annealing : A dramatic pressure decrease of  $\sim 2$  bar was observed under annealing at temperatures very close to the melting point. They thus conjectured that this effect is due to solidification of liquid or glass captured in closed cavities during the growth process [1].

Meanwhile Day and Beamish recently observed an approximately 10% increase in the shear modulus of  $^4\text{He}$  at low temperatures (below 200 mK) [2]. Ray and Hallock found evidence for flow through solid  $^4\text{He}$  in at least some cases [3]. To be specific, Ray and Hallock have conducted experiments that show the first evidence for flow of helium through a region containing solid hcp  $^4\text{He}$  off the melting curve. Their phase diagram appears to have two regions. Samples grown at lower pressures show flow, with flow apparently dependent on sample history, with reduced flow for samples at higher temperature, which is evidence for dependence on temperature. Samples grown at higher pressures show no clear evidence for any such flow for times longer than 10 hours [3]. The temperatures utilized for their work are well above the temperatures at which much attention has been focused, but interesting behavior was seen.

Note also that Clark *et al.* have studied the thermal history of the resonant frequency of a torsional oscillator containing solid  $^4\text{He}$ . They found that the magnitude of the frequency shift that occurs below  $\sim 100$  mK is multi-valued in the low-temperature limit, depending strongly on how the state is prepared [4]. However, Anderson interprets the observed NCRI (nonclassical rotational inertia, please see [4] for the detailed references) as a consequence of vortex liquid and supercurrents flowing around a thermally excited fluctuation of vortices [5]. The subsequent experiments [6] reported the first observations on the time-dependent dissipation when the drive level of a torsional oscillator containing solid  $^4\text{He}$  was abruptly changed. The relaxation of dissipation in solid  $^4\text{He}$  shows rich dynamical behavior including

exponential and logarithmic time-dependent decays, hysteresis, and memory effects. As remarked in [6], their procedure of initiating the oscillation at a high temperature is likely to have brought the sample solid  $^4\text{He}$  to a quasi-equilibrium array of vortices for the drive level at the temperature of measurement. The observed logarithmic time dependence probably arises from the *thermally activated motion* of vortices from one metastable state to another. This process continues throughout the measurement while the sample was maintained at the constant temperature. Just after the drive level has been decreased, the existing vortices are out of equilibrium with the new drive level. The observed undershoot may be a transient excess dissipation owing to the 'wrong' number of vortices. The vortices then must adjust to the new drive level by, say, moving out of the sample. The characteristic time involved in the macroscopic motion of the vortices was then the observed time constant [6]. The motion presumably involves processes occurring both within the sample and at the surface boundaries. The time constant would become shorter as the vortices begin to move more freely. The proposed vortex liquid state [5] appears to occur above about 60 mK. When the vortex liquid 'freezes', the time constant would diverge [6].

Researches mentioned above all imply that the supersolid (material) is not so simple but really complex. We also noticed that as reported by Dyre *et al.* in 1996 for glass-forming molecular liquids the (high-frequency) shear modulus increases as the temperature decreases [7]. The latter resembles that reported in [2] by Day and Beamish. Thus, it's necessary to study the deformation kinetics as well as transport of amorphous and/or glassy material (presumed solid helium to be almost the same) under confined microdomains at rather low temperature regime!

Glasses are amorphous materials of polymeric, metallic, inorganic or organic type. The plastic deformation of amorphous materials and glasses at low temperatures and high strain rates is known to be inhomogeneous and rate-dependent. In fact, the mechanical behavior of amorphous materials such as bulk metallic glasses [7-10] continues to present great theoretical challenges. While dislocations have long been recognized as playing a central role in plasticity of crystalline systems, no counterpart is easily identifiable in disordered matter. In addition, yield and deformation kinetics [11-12] occur very far from equilibrium, where the state of the system may have a complex history dependence.

In recent years, considerable effort was geared towards understanding how glasses respond to shear [12]. Phenomena such as shear thinning and 'rejuvenation' are common when shear

deformation (rate) is imposed. At low temperatures they behave in a brittle elastic manner; at high temperatures, much above the glass transition the behavior is more (rubbery) (viscoelastic). There is a huge drop in modulus when the temperature is increased above the glass transition temperature, indicating a shift in behavior from (glassy) to (rubbery). Because of these peculiar mechanical properties of amorphous materials, the linear theory of viscoelasticity is unable to model closely the observed response and thus there is a need for a non-linear theory of viscoelasticity.

Unlike crystals, glasses also age, meaning that their state depends on their history. When a glass falls out of equilibrium, it evolves over very long time scales. Motivated by the above issues and the interesting characteristics of deformation kinetics at very low temperature we shall study the deformation kinetics in microscopic domain at low enough temperature which is an interesting topic for applications in micro- and nanodomains or the validation in using quantum mechanic formulations [13] where the nonlinear constitutive relations should be adopted.

However, real surfaces are rough at the micro- or even at the meso-scale and the role of surface roughness has been extensively investigated, and opposite conclusions have been reached so far [14-15]. For instance, friction can increase when two opposing surfaces are made smoother (this is the case of cold welding of highly polished metals). On the other hand, friction increases with roughness when interlocking effects among the asperities come into play. This apparent contradiction is due to the effects of length scales, which appear to be of crucial importance in this phenomenon.

From the mechanical point of view, a contact problem involves the determination of the traction distributions transmitted from one surface to the other, in general involving normal pressures and, if friction is present, shear tractions, according to an appropriate set of equalities and inequalities governing the physics of the contact [16]. When there is friction at the contact interface, Coulomb friction behaviour is usually introduced to give the conditions necessary to determine the shear traction distribution. Any point in the contact area must be either in 'stick', or 'slip' condition, and the tangential tractions must behave accordingly. In this paper we shall consider the deformation kinetics of amorphous solid helium at very low temperature in micropores which have radius- or transverse-corrugations along the cross-section. The glassy matter will be treated as a shear-thinning material. To consider the transport of this kind of glass (shear-thinning) material in microdomains, we adopt the

verified model initiated by Cagle and Eyring [9] which was used to study the annealing of glass. To obtain the law of annealing of glass for explaining the too rapid annealing at the earliest time, because the relaxation at the beginning was steeper than could be explained by the bimolecular law, Cagle and Eyring [9] tried a hyperbolic sine law between the shear (strain) rate :  $\dot{\Gamma}$  and (large) shear stress :  $\tau$  and obtained the close agreement with experimental data. This model has sound physical foundation from the thermal activation process (Eyring [10] already considered a kind of (quantum) tunneling which relates to the matter rearranging by surmounting a potential energy barrier; cf., Fig. 1) and thus it might also resolve the concern raised by Anderson [5] for the thermal noises to the superflow of vortex liquid (i.e., the supersolid helium).

With this model we can associate the (glassy) matter with the momentum transfer between neighboring atomic clusters on the microscopic scale and reveals the atomic interaction in the relaxation of flow with (viscous) dissipation.

The outline of this short paper is as follows. Section 2 describes the general physical formulations of the framework. In this Section, explicit derivations for the glassy deformation kinetics are introduced based on a microscopic model proposed by Eyring [10]. The boundary perturbation technique [17] will be implemented, too. In the third Section, we consider the very-low temperature limit of our derived solutions which are highly temperature as well as activation energy dependent at rather low temperature regime. Relevant results and discussion are given therein.

## II. THEORETICAL FORMULATIONS

The beginnings of theoretical molecular mechanisms of deformation in amorphous materials and glass are as old as the subject of atomic mechanisms of deformation and yield in metals. The first specific molecular mechanism of deformation for amorphous materials and glass was published by Eyring [10] and later, Taylor [18] published the model of an edge dislocation to account for the plastic deformation in metals. However, whilst the theory of dislocations and crystal defects has become a major stream in the science of solid state, the corresponding effort applied to this problem in amorphous materials must be considered rather small by comparison.

The molecular theory of deformation kinetics came from a different stream of science than

that of structure and motion of crystal defects (in particular dislocations). Its roots stretch to the developmental stages of theories of chemical reactions and thermodynamic description of their temperature dependence, culminating in the key formulation by Arrhenius of the equation for reaction rates. By the beginning of this century the concept of activation entropy was included in the model, and it was considered that molecules go both in the forward direction (product state) and in the backward direction (reactant state).

The development of statistical mechanics, and later quantum mechanics, led to the concept of the potential energy surface. This was a very important step in our modern understanding of atomic models of deformation. Eyring's contribution to this subject was the formal development of the transition state theory which provided the basis for deformation kinetics, as well as all other thermally activated processes, such as crystallisation, diffusion, polymerisation. etc. [10]

The motion of atoms is represented in the configuration space; on the potential surface the stable molecules are in the valleys, which are connected by a pass that leads through the saddle point. An atom at the saddle point is in the transition (activated) state. Under the action of an applied stress the forward velocity of a (plastic) flow unit is the net number of times it moves forward, multiplied by the distance it jumps. Eyring proposed a specific molecular model of the amorphous structure and a mechanism of deformation kinetics [10]. With reference to this idea, this mechanism results in a (shear) strain rate given by

$$\dot{\Gamma} = 2 \frac{V_h}{V_m} \frac{k_B T}{h} \exp\left(\frac{-\Delta E}{k_B T}\right) \sinh\left(\frac{V_h \tau}{2 k_B T}\right) \quad (1)$$

where

$$V_h = \lambda_2 \lambda_3 \lambda, \quad V_m = \lambda_2 \lambda_3 \lambda_1,$$

$\lambda_1$  is the perpendicular distance between two neighboring layers of molecules sliding past each other,  $\lambda$  is the average distance between equilibrium positions in the direction of motion,  $\lambda_2$  is the distance between neighboring molecules in this same direction (which may or may not equal  $\lambda$ ),  $\lambda_3$  is the molecule to molecule distance in the plane normal to the direction of motion, and  $\tau$  is the local applied stress,  $\Delta E$  is the activation energy,  $h$  is the Planck constant,  $k_B$  is the Boltzmann constant,  $T$  is the temperature,  $V_h$  is the activation volume for the molecular event [9-10]. The deformation kinetics of the chain is envisaged as the propagation of kinks in the molecules into available holes. In order for the motion of the kink to result in a plastic flow, it must be raised (energised) into the activated state and

pass over the saddle point. This was the earliest molecular theory of yield behaviour in amorphous materials, and Eyring presented a theoretical framework which formed the basis of many subsequent considerations.

Solving Eqn. (1) for the force or  $\tau$ , one obtains:

$$\tau = \frac{2k_B T}{V_h} \sinh^{-1}\left(\frac{\dot{\Gamma}}{B}\right), \quad (2)$$

which in the limit of small  $(\dot{\Gamma}/B)$  reduces to Newton's law for viscous deformation kinetics. We consider a steady deformation kinetics of the glassy material in a wavy-rough microtube of  $r_o$  (in mean-averaged outer radius) with the outer wall being a fixed wavy-rough surface :  $r = r_o + \epsilon \sin(k\theta)$  where  $\epsilon$  is the amplitude of the (wavy) roughness, and the wave number :  $k = 2\pi/L$  ( $L$  is the wave length). The schematic is illustrated in Fig. 2. Firstly, this material can be expressed as [9-10,14]  $\dot{\Gamma} = \dot{\Gamma}_0 \sinh(\tau/\tau_0)$ , where  $\dot{\Gamma}$  is the shear rate,  $\tau$  is the shear stress, and

$$\dot{\Gamma}_0 \equiv B = \frac{2k_B T}{h} \frac{V_h}{V_m} \exp\left(\frac{-\Delta E}{k_B T}\right), \quad (3)$$

is a function of temperature with the dimension of the shear rate,

$$\tau_0 = \frac{2k_B T}{V_h} \quad (4)$$

is the referenced (shear) stress, (for small shear stress  $\tau \ll \tau_0$ , the linear dashpot constitutive relation is recovered and  $\tau_0/\dot{\Gamma}_0$  represents the viscosity of the material). In fact, the force balance gives the shear stress at a radius  $r$  as  $\tau = -(r dp/dz)/2$ .  $dp/dz$  is the pressure gradient along the tube-axis or  $z$ -axis direction.

Introducing the forcing parameter  $\Pi = -(r_o/2\tau_0)dp/dz$  then we have  $\dot{\Gamma} = \dot{\Gamma}_0 \sinh(\Pi r/r_o)$ .

As the (shear) strain rate is

$$\dot{\Gamma} = \frac{du}{dr} \quad (5)$$

( $u$  is the rate of deformation (or velocity) in the longitudinal ( $z$ -)direction of the microtube), after integration, we obtain

$$u = u_s + \frac{\dot{\Gamma}_0 r_o}{\Pi} [\cosh \Pi - \cosh(\frac{\Pi r}{r_o})], \quad (6)$$

here,  $u_s$  is the rate of deformation or velocity over the surfaces of the microtube, which is determined by the boundary condition. We noticed that a general boundary condition for material deformation kinetics over a solid surface was proposed (cf., e.g., [14]) as

$$\delta u = L_s^0 \dot{\Gamma} \left(1 - \frac{\dot{\Gamma}}{\dot{\Gamma}_c}\right)^{-1/2}, \quad (7)$$

where  $\delta u$  is the rate of deformation (or velocity) jump over the solid surface,  $L_s^0$  is a constant slip length and  $\dot{\Gamma}_c$  is the critical shear rate at which the slip length diverges. The value of  $\dot{\Gamma}_c$  is a function of the corrugation of interfacial energy. We remind the readers that this expression is based on the assumption of the shear rate over the solid surface being much smaller than the critical shear rate of  $\dot{\Gamma}_c$ .  $\dot{\Gamma}_c$  represents the maximum shear rate the material can sustain beyond which there is no additional momentum transfer between the wall and material-flow molecules. How generic this behavior is and whether there exists a comparable scaling for glassy or amorphous materials remain open questions.

At small pressure gradient, the shear-thinning matter behaves like a Newtonian flow, while at high pressure gradient, the shear-thinning matter flows in a plug-flow type. Such a behavior is due to the shear thinning of the material, i.e., the higher the shear rate is, the smaller is the (plastic) flow resistance [7]. On the microscale, this shear-thinning matter can bridge the Newtonian deformation kinetics to that of the pluglike type and offers us a mechanistic model to study the deformation kinetics in micro- and even nanodomains using the technique of continuum mechanics.

With the boundary condition from (cf., e.g., [18]), we shall derive the rate of deformation (or velocity) field or deformation kinetics along the wavy-rough microtube below using the boundary perturbation technique (cf. [23]) and dimensionless analysis. We firstly select the hydrodynamical diameter  $L_r$  to be the characteristic length scale and set

$$r' = r/L_r, \quad R_o = r_o/L_r, \quad \epsilon' = \epsilon/L_r. \quad (8)$$

After this, for simplicity, we drop all the primes. It means, now,  $r$ ,  $R_o$ ,  $R_i$ , and  $\epsilon$  become dimensionless. The wall is prescribed as  $r = R_o + \epsilon \sin(k\theta)$ , and the presumed fully-developed plastic flow is along the  $z$ -direction (microtube-axis direction). Along the confined (wavy) boundaries, we have the strain rate

$$\dot{\Gamma} = \left( \frac{du}{dn} \right)_{\text{on surface}}, \quad (9)$$

where,  $n$  means the normal. Let the rate of deformation  $u$  be expanded in  $\epsilon$  :

$$u = u_0 + \epsilon u_1 + \epsilon^2 u_2 + \cdots, \quad (10)$$

and on the boundary, we expand  $u(r_0 + \epsilon dr, \theta (= \theta_0))$  into

$$u(r, \theta)|_{(r_0 + \epsilon dr, \theta_0)} = u(r_0, \theta) + \epsilon [dr u_r(r_0, \theta)] + \epsilon^2 \left[ \frac{dr^2}{2} u_{rr}(r_0, \theta) \right] + \cdots =$$

$$\{u_{slip} + \frac{\dot{\Gamma} R_o}{\Pi} \cosh(\frac{\Pi \bar{r}}{R_o})|_{r=R_o+\epsilon \sin(k\theta)}, \quad r_0 \equiv R_o; \quad (11)$$

where the subscript means the partial differentiation (say,  $u_r \equiv \partial u / \partial r$ ) and

$$u_{slip}|_{\text{on surface}} = L_s^0 \dot{\Gamma} [(1 - \frac{\dot{\Gamma}}{\dot{\Gamma}_c})^{-1/2}]|_{\text{on surface}}, \quad (12)$$

$$u_{slip_0} = L_s^0 \dot{\Gamma}_0 [\sinh \Pi (1 - \frac{\dot{\Gamma}_0 \sinh \Pi}{\dot{\Gamma}_c})^{-1/2}]. \quad (13)$$

Now, on the outer wall (cf., e.g., [23]), the (shear) strain rate

$$\begin{aligned} \dot{\Gamma} = \frac{du}{dn} = \nabla u \cdot \frac{\nabla(r - R_o - \epsilon \sin(k\theta))}{|\nabla(r - R_o - \epsilon \sin(k\theta))|} &= [1 + \epsilon^2 \frac{k^2}{r^2} \cos^2(k\theta)]^{-\frac{1}{2}} [u_r|_{(R_o+\epsilon dr, \theta)} - \\ &\epsilon \frac{k}{r^2} \cos(k\theta) u_\theta|_{(R_o+\epsilon dr, \theta)}] = u_{0r}|_{R_o} + \epsilon [u_{1r}|_{R_o} + u_{0rr}|_{R_o} \sin(k\theta) - \\ &\frac{k}{r^2} u_{0\theta}|_{R_o} \cos(k\theta)] + \epsilon^2 [-\frac{1}{2} \frac{k^2}{r^2} \cos^2(k\theta) u_{0r}|_{R_o} + u_{2r}|_{R_o} + u_{1rr}|_{R_o} \sin(k\theta) + \\ &\frac{1}{2} u_{0rrr}|_{R_o} \sin^2(k\theta) - \frac{k}{r^2} \cos(k\theta) (u_{1\theta}|_{R_o} + u_{0\theta r}|_{R_o} \sin(k\theta))] + O(\epsilon^3). \end{aligned} \quad (14)$$

Considering  $L_s^0 \sim R_o \gg \epsilon$  case, we presume  $\sinh \Pi \ll \dot{\Gamma}_c / \dot{\Gamma}_0$  so that we can approximately replace  $[1 - (\dot{\Gamma}_0 \sinh \Pi) / \dot{\Gamma}_c]^{-1/2}$  by  $[1 + \dot{\Gamma}_0 \sinh \Pi / (2\dot{\Gamma}_c)]$ . With equations (6),(7),(9), (10), (11) and (14), using the definition of the (shear) strain rate  $\dot{\Gamma}$ , we can derive the rate of deformation (or velocity) field up to the second order. The key point is to firstly obtain the slip rate of deformation (or velocity) along the wavy boundaries or surfaces.

After lengthy mathematical manipulations and using  $(1 - \dot{\Gamma} / \dot{\Gamma}_c)^{-1/2} \approx 1 + \dot{\Gamma} / (2\dot{\Gamma}_c)$ ,

$$u_0 = -\frac{\dot{\Gamma}_0 R_o}{\Pi} [\cosh(\frac{\Pi r}{R_o}) - \cosh \Pi] + u_{slip_0}, \quad (15)$$

$$u_1 = \dot{\Gamma}_0 \sin(k\theta) \sinh \Pi + u_{slip_1}, \quad (16)$$

we have

$$\begin{aligned} u_{slip} = L_s^0 \{ [-u_{0r} (1 - \frac{u_{0r}}{2\dot{\Gamma}_c})]|_{r=R_o} + \epsilon [-u_f (1 - \frac{u_{0r}}{\dot{\Gamma}_c})]|_{r=R_o} + \epsilon^2 [\frac{u_f^2}{2\dot{\Gamma}_c} - u_{sc} (1 - \frac{u_{0r}}{\dot{\Gamma}_c})]|_{r=R_o} \} = \\ u_{slip_0} + \epsilon u_{slip_1} + \epsilon^2 u_{slip_2} + O(\epsilon^3) \end{aligned} \quad (17)$$

where

$$u_{0r} = -\dot{\Gamma}_0 \sinh(\frac{\Pi}{R_o} r), \quad (18)$$

$$u_{0rr} = -\dot{\Gamma}_0 \frac{\Pi}{R_o} \cosh(\frac{\Pi}{R_o} r), \quad (19)$$

$$u_{0rrr} = -\dot{\Gamma}_0 \frac{\Pi^2}{R_o^2} \sinh\left(\frac{\Pi}{R_o} r\right), \quad (20)$$

$$u_f = u_{1_r} + u_{0_{rr}} \sin(k\theta) - \frac{k}{r^2} \cos(k\theta) u_{0_\theta} = -\frac{\Pi}{R_o} \dot{\Gamma}_0 \cosh\left(\frac{\Pi}{R_o} r\right) \sin(k\theta), \quad (21)$$

and

$$u_{sc} = -\frac{k^2}{2r^2} \cos^2(k\theta) u_{0_r} + \frac{1}{2} u_{0_{rrr}} \sin^2(k\theta) = \frac{1}{2} \dot{\Gamma}_0 \left[ \frac{k^2}{2r^2} \cos^2(k\theta) - \frac{\Pi^2}{R_o^2} \sin^2(k\theta) \right] \sinh\left(\frac{\Pi}{R_o} r\right). \quad (22)$$

Thus, at  $r = R_o$ , up to the second order,

$$u_{slip} \equiv u_s = L_s^0 \dot{\Gamma}_0 \sinh \Pi \left(1 + \frac{K_0}{2}\right) + \epsilon \dot{\Gamma}_0 \sin(k\theta) \left[ \sinh \Pi + \frac{\Pi}{R_o} L_s^0 \cosh \Pi (1 + K_0) \right] + \epsilon^2 L_s^0 \frac{\dot{\Gamma}_0}{2} \left\{ \left[ \frac{\Pi \cosh \Pi}{R_o L_s^0} \sin^2(k\theta) - \frac{k^2}{R_o^2} \cos^2(k\theta) + \frac{\Pi^2}{R_o^2} \sin^2(k\theta) \right] \sinh \Pi (1 + K_0) + \frac{\Pi^2}{R_o^2} \frac{\dot{\Gamma}_0}{\dot{\Gamma}_c} \cosh^2 \Pi \sin^2(k\theta) \right\}, \quad (23)$$

where

$$K_0 = 1 + (\dot{\Gamma}_0 \sinh \Pi) / \dot{\Gamma}_c \quad (24)$$

From the rate of deformation (or velocity) fields (up to the second order), we can integrate them with respect to the cross-section to get the volume (plastic) flow rate ( $Q$ , also up to the second order here).

$$Q = \int_0^{\theta_p} \int_{R_o}^{R_o + \epsilon \sin(k\theta)} u(r, \theta) r dr d\theta = Q_{smooth} + \epsilon Q_{p_0} + \epsilon^2 Q_{p_2}. \quad (25)$$

### III. RESULTS AND DISCUSSION

We firstly check the roughness effect upon the shearing characteristics because there are no available experimental data and numerical simulations for the same geometric configuration (microscopic tubes with wavy corrugations in transverse direction). With a series of forcings (due to imposed pressure gradients) :  $\Pi \equiv R_o(-dp/dz)/(2\tau_0)$ , we can determine the enhanced shear rates ( $d\Gamma/dt$ ) due to forcings. From equation (5), we have (up to the first order)

$$\frac{d\Gamma}{dt} = \frac{d\Gamma_0}{dt} \left[ \sinh \Pi + \epsilon \sin(k\theta) \frac{\Pi}{R_o} \cosh \Pi \right]. \quad (26)$$

The calculated results are demonstrated in Figs. 3 and 4. The parameters are fixed below (the orientation effect :  $\sin(k\theta)$  is fixed here).  $r_o$  (the mean outer radius) is selected as the same as the slip length  $L_s^0 = 100$  nm. The amplitude of wavy roughness is  $\epsilon = 0.04, 0.07, 0.1$ ,

the Boltzmann constant ( $k_B$ ) is  $1.38 \times 10^{-23}$  Joule/ $^{\circ}\text{K}$ , and the Planck constant ( $h$ ) is  $6.626 \times 10^{-34}$  Joule  $\cdot$  s.

In each panel, the inner curve is the relevant boundary of the tube or the geometric part of the presentation. The distance between the inner and corresponding outer curves is the calculated physical shear rate :  $\dot{\Gamma}$ . We can observe once the temperature ( $T$ ) changes a little from  $0.1^{\circ}$  to  $0.15^{\circ}$ , the enhancement of  $\dot{\Gamma}$  becomes at least three orders of magnitude (for  $\Pi = 1$ , the activation energy :  $3 \times 10^{-23}$  Joules). Even at very low temperature Fig. 4 gives very large strain rates which are required to obtain the necessary strain for plastic deformation. Thus, the constitutive relations is highly nonlinear at rather low temperature regime [9]. It is worth pointing out that the Eyring model requires the interaction between atoms in the direction perpendicular to the shearing direction for the momentum transfer. This might explain why our result is orientation dependent. The effect of wavy-roughness will be significant once the forcing ( $\Pi$ ) is rather large (the maximum is of the order of magnitude of  $\epsilon[\Pi \tanh(\Pi)/R_o]$ ).

To be specific, we can illustrate the shear rate ( $\dot{\Gamma}$ ) with respect to the temperature ( $T$ ) once we calculate  $\dot{\Gamma}_0$  as the latter is temperature dependent (but presumed roughness independent here) which could be traced from equation (1). This is shown in Fig. 5.

Note that, based on the rate-state Eyring model (of stress-biased thermal activation), structural rearrangement is associated with a single energy barrier (height)  $E$  that is lowered or raised linearly by a (shear) yield stress  $\tau$ . If the transition rate is proportional to the plastic (shear) strain rate (with a constant ratio :  $C_0$ ;  $\dot{\Gamma} = C_0 R_t$ ,  $R_t$  is the transition rate in the direction aided by stress), we have  $\tau = E/V^* + (k_B T/V^*) \ln(\dot{\Gamma}/C_0 \nu_0)$  or

$$\tau = \frac{E}{V^*} + \left(\frac{k_B T}{V^*}\right) \ln\left(\frac{|\dot{\tau}| V^*}{\nu_0 k_B T}\right), \quad (27)$$

where  $V^* \equiv V_h$  is a constant called the activation volume,  $k_B$  is the Boltzmann constant,  $T$  is the temperature,  $\nu_0$  is an attempt frequency or transition rate [8,25], and  $\dot{\tau}$  is the stress rate. Normally, the value of  $V^*$  is associated with a typical volume required for a molecular shear rearrangement. Thus, if there is a rather-small (plastic) flow (of the glass) at low temperature environment then it could be related to a barrier-overcoming or tunneling for shear-thinning matter along the wavy-roughness (geometric valley and peak served as atomic potential surfaces) in cylindrical micropores when the wavy-roughness is present. Once the geometry-tuned potentials (energy) overcome this barrier, then the tunneling (spontaneous

transport) inside wavy-rough cylindrical micropores occurs.

To examine the behavior of the shear rate at low temperature regime, we calculate  $\dot{\Gamma}_0$  and  $\dot{\Gamma}$  ( $C_0\nu_0 = 5 \times 10^{10} \text{ s}^{-1}$ ) with respect to the temperature  $T$  and show the results in Fig. 5. For a selected activation energy :  $5 \times 10^{-24}$  Joule or  $\sim 10^{-5}$  eV (a little bit smaller than the binding energy of  $^3\text{He}$ ), we can find a sharp decrease of shear rates around  $T \sim 0.01^\circ\text{K}$ . Below this temperature, there might be nearly frictionless transport of glassy matter. Note also that, according to Cagle and Eyring [8],  $V^* = 3V\delta\Gamma/2$  for certain material during an activation event, where  $V$  is the deformation volume,  $\delta\Gamma$  is the increment of shear strain. If we select a (fixed) temperature, say,  $T = 0.1^\circ\text{K}$ , then from the expression of  $\tau_0$ , we can obtain the shear stress  $\tau$  corresponding to above forcings ( $\Pi$ ) :

$$\tau = \tau_0 \sinh^{-1}[\sinh(\Pi) + \epsilon \sin(k\theta) \frac{\Pi}{R_o} \cosh(\Pi)]. \quad (28)$$

There is no doubt that the orientation effect ( $\theta$ ) is also present for deformation kinetics of amorphous matter. For illustration (shown in Fig. 6), we only consider the maximum case :  $|\sin(k\theta)| = 1$ . The trend of enhancement due to  $\Pi$  (pressure-forcing) and  $\epsilon$  (roughness) is similar to those presented in Figs. 3 and 4. We remind the readers that, due to the appearance of  $\tau_0$ , we fix the temperature to be  $0.1^\circ\text{K}$  and the activation volume :  $10^{-25} \text{ m}^3$ . In fact, as shown in Fig. 6, the calculated (shear) stress (which is directly linked to the resistance of the glassy matter) also shows a sudden decrease around  $T \sim 0.05^\circ\text{K}$  especially for the case of ( $C_0\nu_0 = 2 \times 10^9 \text{ s}^{-1}$ ). Here, the activation volume ( $V^*$  or  $V_h$ ) is selected as  $0.2 \text{ nm}^3$  [19]. Thus, the nearly frictionless transport of the glassy fluid at low temperature environment (relevant to the supersolidity, cf. [20]) could be related to a barrier-overcoming or tunneling for shear-thinning matter along the wavy-roughness (geometric valley and peak served as atomic potential surfaces) in cylindrical micropores when the wavy-roughness is present. Once the geometry-tuned potentials (energy) overcome this barrier, then the tunneling (almost frictionless transport) inside wavy-rough cylindrical micropores occurs.

We also noticed that, as described in [9-10], mechanical loading lowers energy barriers, thus facilitating progress over the barrier by random thermal fluctuations. The simplified Eyring model approximates the loading dependence of the barrier height as linear. This Eyring model, with this linear barrier height dependence on load, has been used over a large fraction of the last century to describe the response of a wide range of systems and underlies modern approaches to sheared glasses. The linear dependence will always correctly describe

small changes in the barrier height, since it is simply the first term in the Taylor expansion of the barrier height as a function of load. It is thus appropriate when the barrier height changes only slightly before the system escapes the local energy minimum. This situation occurs at higher temperatures; for example, Newtonian deformation kinetics is obtained in the Eyring model in the limit where the system experiences only small changes in the barrier height before thermally escaping the energy minimum. As the temperature decreases, larger changes in the barrier height occur before the system escapes the energy minimum (giving rise to, for example, non-Newtonian deformation kinetics). In this regime, the linear dependence is not necessarily appropriate, and can lead to inaccurate modelling. This explains why we should adopt the hyperbolic sine law [9-10] to treat the glassy matter.

To be specific, our results are rather sensitive to the temperature ( $T$ ) and the activation energy. Fig. 7 shows especially the temperature dependence of the forcing parameter ( $\Pi$ ) if  $dp/dz$  is prescribed (say, around  $6 \times 10^{10}$  Pa/m) and the activation volume is  $0.2 \text{ nm}^3$  ( $r_o = 100 \text{ nm}$ ). We can observe that once  $T$  increases  $\Pi$  decreases.  $\dot{\Gamma}$  calculated using prescribed  $\Pi$  and using directly  $T$  also differs.

Finally, we present the calculated maximum velocity (unit : m/s) with respect to the temperature in Fig. 8. Geometric parameters :  $r_o$  and the activation volume are the same as those in Fig. 7 and the roughness amplitude  $\epsilon = 0.02, 0.05R_o$ . We consider the effect of the activation energy :  $1.5 \times 10^{22}$  and  $2 \times 10^{22}$  Joule. Around  $T \sim 0.35^\circ\text{K}$ , the maximum velocity (of the glassy matter) either keeps decreasing as the temperature increases for larger activation energy or instead increases as the temperature increases for smaller activation energy! The results presented in Fig. 8 might be related to the microscopic origin for physical aging or effects of thermal history [21] and indeterminate solutions discussed in [22]. The latter observation might be related to the argues raised in [23] for the annealing process of solid helium at similar low temperature environment if we treat the solid helium to be glassy at low temperature regime. On the other hand, we like to remind the readers about the role of roughness again. If  $^4\text{He}$  is isotropic (prepared), and the impurity of  $^3\text{He}$  distribution was added or mixed into  $^4\text{He}$  quite regularly (equally-distributed). It's possible that the role of  $^3\text{He}$  [24] plays under certain selected activation energy and activation volume is qualitatively the same as that of the roughness here. In general, as commented in [25] : *An understanding of the NCRI effect may therefore require explicit treatment of the effects of strain on the crystal properties ... We have used a narrow x-ray beam to study the defects in  $^4\text{He}$  crystals,*

and we find crystals contain a microstructure of mosaic regions consistent with small angle grain boundaries  $\dots$ , our presentation here is crucial to the understanding of strain upon the solid helium at rather low temperature regime once the solid helium is presumed to be glassy (cf. [26] for the detailed references) within confined microdomains. To give our approach another comparison with the transport data in [3], e.g., with the same temperature 0.4 K as in Fig. 4 of [3], once we set the activation energy ( $\Delta E$ ) to be  $1.0 \times 10^{-22}$  Joule (or  $\sim 10^{-3}$  eV; cf. Fig. 3 in [27]), the radius to be  $\sim 1\mu\text{m}$ , with other parameters the same as those in Fig. 8 above, then we have the maximum velocity being around  $100\mu\text{m}/\text{sec}$  which is almost the same as that estimated in [3] (where the uniform flow was presumed and the fraction of the helium that can flow is  $2.5 \times 10^{-6}$ ). This is illustrated in Fig. 9.

#### IV. CONCLUSIONS

To conclude in brief, we analytically obtain a class of temperature as well as activation energy dependent fields of the rate of deformation for glassy material (like solid helium) in microscopically confined wavy-rough domain at very low temperature regime. The effects of wavy corrugation upon the confined deformation kinetics at very-low temperature are clearly illustrated. It is found that there exist almost frictionless plastic flow fields for the rate of deformation of glassy material inside cylindrical micropores at very low temperature once the micropore surface is wavy-rough and the activation energy is prescribed. Once the temperature, activation volume, and geometry are fixed, the increase of activation energy instead reduces significantly the (maximum) rate of deformation of the glassy matter. The critical rate of deformation is proportional to the (referenced) shear rate, the slip length, the orientation and the amplitude of the wavy-roughness as illustrated above. Our approaches can recover those transport results reported in [3] for the same physical parameters.

#### Acknowledgement.

The author is partially supported by the 2007-Hebei-NU Starting Funds for Scientific Researcher. The author thanks the hospitality for the Visiting-Scholar Program of the Chern Shiing-Shen Institute of Mathematics, Nankai University.

- 
- [1] V.N. Grigor'ev, V.A. Maidanov, V.Yu. Rubanskii, S.P. Rubets, E.Ya. Rudavskii, A.S. Rybalko, Ye.V. Syrnikov and V.A. Tikhii, Phys. Rev. B **76**, 224524 (2007).
  - [2] J. Day and J. Beamish, Nature **450**, 853 (2007).
  - [3] M.W. Ray and R.B. Hallock, Phys. Rev. Lett. **100**, 235301 (2008).
  - [4] A.C. Clark, J.D. Maynard and M.H.W. Chan, Phys. Rev. B **77**, 184513 (2008).
  - [5] P.W. Anderson, Nature Phys. **3**, 160 (2007).
  - [6] Y. Aoki, M.C. Keiderling and H. Kojima, Phys. Rev. Lett. **100**, 215303 (2008).
  - [7] J.C. Dyre, N.B. Olsen and T. Christensen, Phys. Rev. B **53**, 2171 (1996).
  - [8] R.N. Haward and R.J. Young, The Physics of Glassy Polymers (Chapman and Hall, London, 1997).
  - [9] F.W. Cagle Jr. and H. Eyring, J. Appl. Phys. **22**, 771 (1951).
  - [10] H. Eyring, J. Chem. Phys. **4**, 283 (1936). A. Tobolsky and H. Eyring, J. Chem. Phys. **11**, 125 (1943).
  - [11] A.J. Liu and S.R. Nagel, Jamming and Rheology (Taylor & Francis, London, 2001).
  - [12] T.K. Haxton and A.J. Liu, Phys. Rev. Lett. **99**, 195701 (2007).
  - [13] J.F. Bell, Int. J. Plast. **1**, 3 (1985). J.F. Bell, Int. J. Plast. **4**, 127 (1988).
  - [14] Z. K.-H. Chu, arXiv:0707.2828. Z. K.-H. Chu, Ann. Phys. (Berlin) **17**, 343 (2008).
  - [15] R. van Tijum, W.P. Vellinga and J.Th.M. De Hosson, Acta Mater. **55**, 2757 (2007).
  - [16] K.L. Johnson, Proc. Royal Soc. London A **453**, 163 (1997).
  - [17] K.-H. W. Chu, J. Phys. Chem. B **112**, 3019 (2008). W. K.-H. Chu, Z. Angew. Math. Phys. **47**, 591 (1996).
  - [18] G.I. Taylor, J. Inst. Met. **62**, 307 (1938).
  - [19] F.M. Capaldi, M.C. Boyce and G.C. Rutledge, Polymer **45**, 1391 (2004).
  - [20] Y. Pomeau and S. Rica, Phys. Rev. Lett. **72**, 2426 (1994).
  - [21] A. Wypych, E. Duval, G. Boiteux, J. Ulanski, L. David and A. Mermet, Polymer **46**, 12523 (2005).
  - [22] T.B. Stoughton and J.W. Yoon, Int. J. Plast. **24**, 583 (2008).
  - [23] A. Penzev, Y. Yasuta and M. Kubota, J. Low Temp. Phys. **148**, 677 (2007).

- [24] N. Mulders, J.T. West, M.H.W. Chan, C.N. Kodituwakku, C.A. Burns and L.B. Lurio, Arxiv: 0808.2871.
- [25] C.A. Burns, N. Mulders, L. Lurio, M.H.W. Chan, A. Said1, C.N. Kodituwakku and P.M. Platzman, Arxiv: 0808.2872.
- [26] N. Prokofev, Adv. Phys. 56, 381 (2007). S. Balibar and F. Caupin, J. Phys.: Condens. Matter **20**, 173201 (2008). A. Andreev, JETP Lett. **85**, 585 (2007). A.S.C. Rittner and J.D. Reppy, arXiv:0807.2183.
- [27] Z. K.-H. Chu, arXiv:0805.0033.

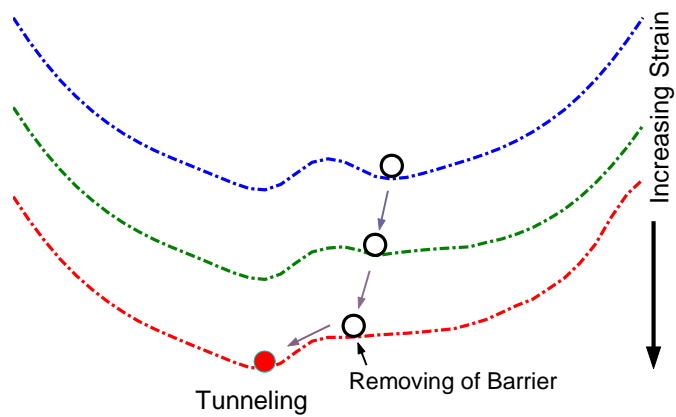


Fig. 1 Increasing strain causes a local energy minimum to flatten until it disappears (removing of energy barrier or quantum-like tunneling). The structural contribution to the shear stress is shear thinning.

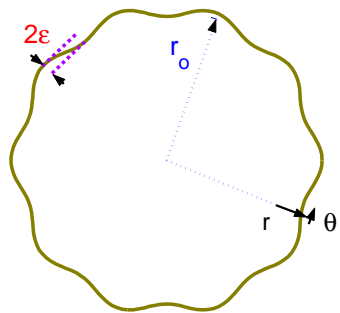


Fig. 2. Schematic of a cylindrical micropore.  $\epsilon$  is the amplitude of small wavy-roughness.

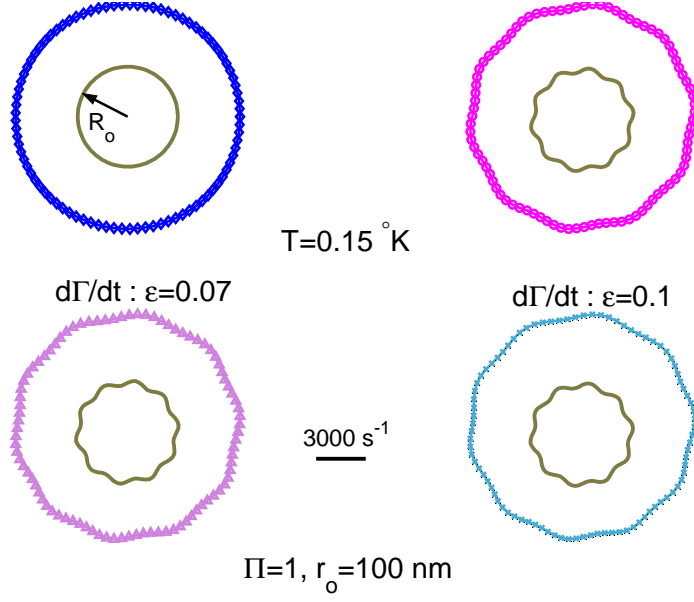


Fig. 3. Comparison of the shear rate ( $\dot{\Gamma}$ ) of glassy matter in smooth microtubes and wavy-rough microtubes for  $k = 10$ ,  $\epsilon = 0.0, 0.04, 0.07, 0.1$  with  $r_o=100$  nm.  $\dot{\Gamma}_c/\dot{\Gamma}_0 = 10$  and  $L_s^0 = r_o$ .  $k$  is the wave number and  $\epsilon$  is the amplitude of the wavy-roughness.  $T$  is the temperature. The solid-line length represents the scale of  $\dot{\Gamma} = 10s^{-1}$ .

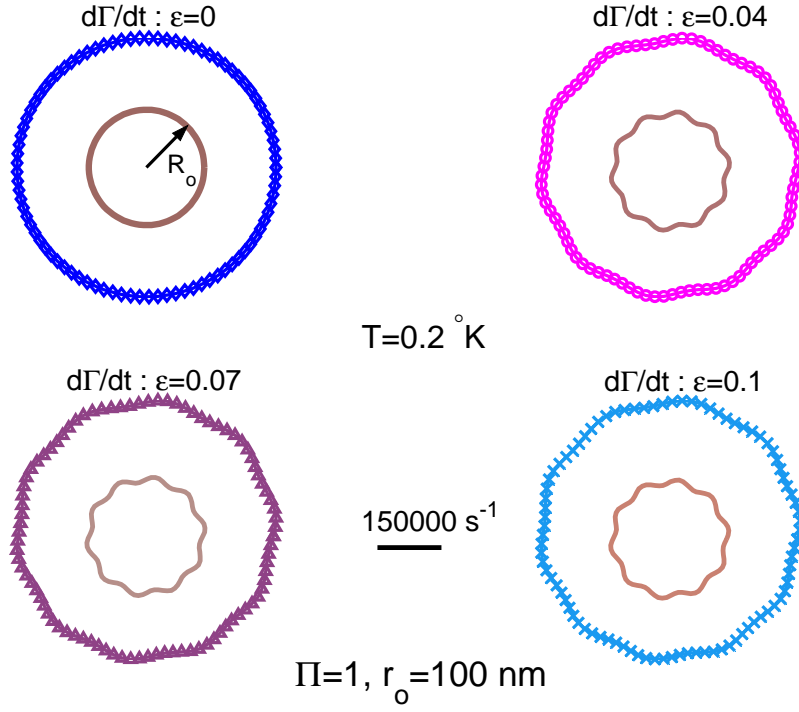


Fig. 4. Comparison of the shear rate ( $\dot{\Gamma}$ ) of glassy matter in smooth microtubes and wavy-rough microtubes for  $k = 10$ ,  $\epsilon = 0.0, 0.04, 0.07, 0.1$  with  $r_o = 100$  nm.  $\dot{\Gamma}_c/\dot{\Gamma}_0 = 10$  and  $L_s^0 = r_o$ .  $k$  is the wave number and  $\epsilon$  is the amplitude of the wavy-roughness.  $T$  is the temperature. The solid-line length represents the scale of  $\dot{\Gamma} = 3000s^{-1}$ . As the temperature increases a little,  $\dot{\Gamma}$  increases significantly.

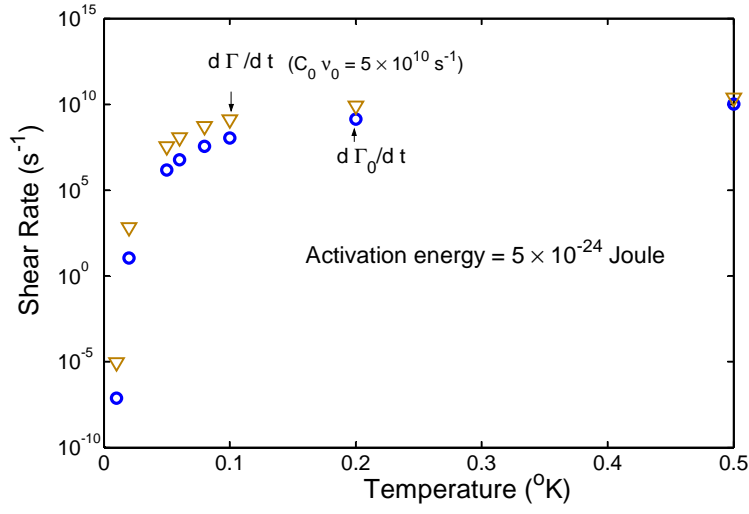


Fig. 5 Comparison of calculated shear (strain) rates using an activation energy  $5 \times 10^{-24}$  Joule or  $\sim 10^{-5}$  eV. There is a sharp decrease of shear rate around  $T \sim 0.01^{\circ}K$ .

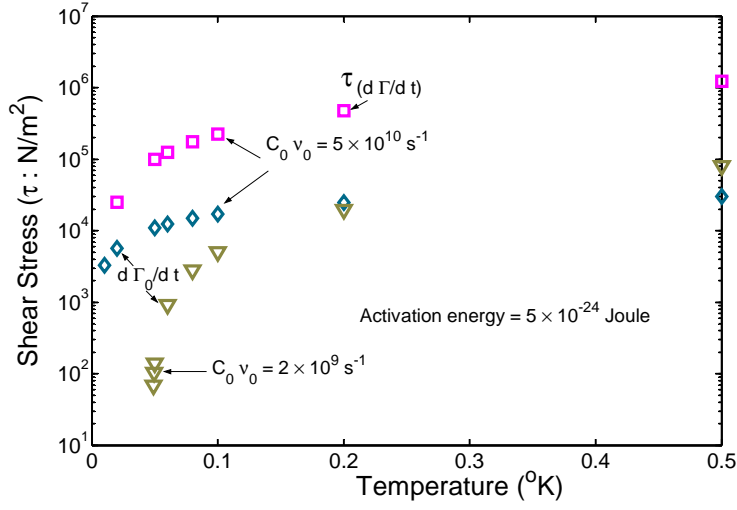


Fig. 6 Comparison of calculated (shear) stresses using an activation energy  $5 \times 10^{-24}$  Joule or  $\sim 10^{-5}$  eV. There is a sharp decrease of shear stress around  $T \sim 0.05^\circ\text{K}$  for  $C_0\nu_0 = 2 \times 10^9 \text{ s}^{-1}$ . Below  $0.05^\circ\text{K}$ , the transport of glassy matter is nearly frictionless.

$\nu_0$  is an attempt frequency or transition rate [10,19].

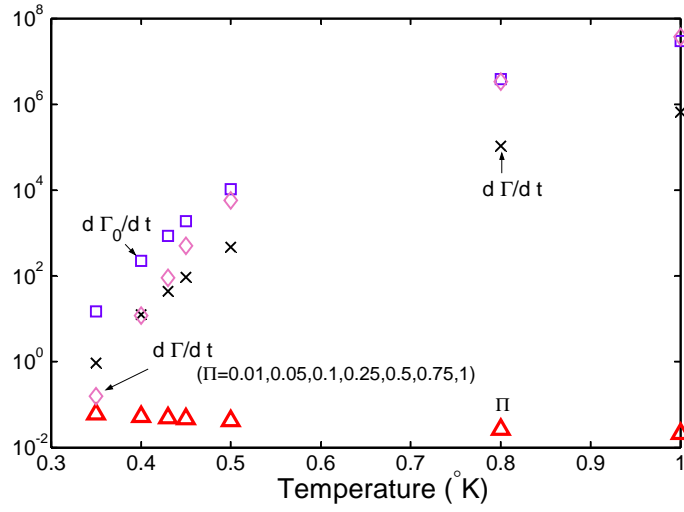


Fig. 7 Comparison of calculated shear (strain) rates using an activation energy  $10^{-22}$  Joule or  $\sim 10^{-3}$  eV. The temperature ( $T$ ) dependence of  $\Pi$  (forcing) is also demonstrated. Forcing ( $\Pi$ ) decreases as the temperature ( $T$ ) increases.  $\dot{\Gamma}$  (mark : diamond) calculated using prescribed  $\Pi$  is different from that (mark : cross) using directly  $T$  (temperature).

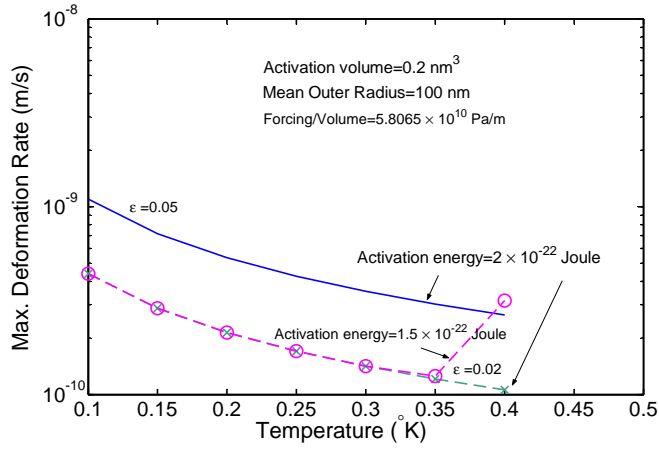


Fig. 8 Comparison of calculated (maximum) velocity (unit : m/s) using two activation energies  $1.5 \times 10^{-22}$  and  $2 \times 10^{-22}$  Joule. Around  $T \sim 0.35^\circ\text{K}$ , the monotonic trend of velocity (or deformation rate) bifurcates as the temperature increases.

$$r_o = 100 \text{ nm and } \epsilon = 0.02, 0.05 R_o.$$

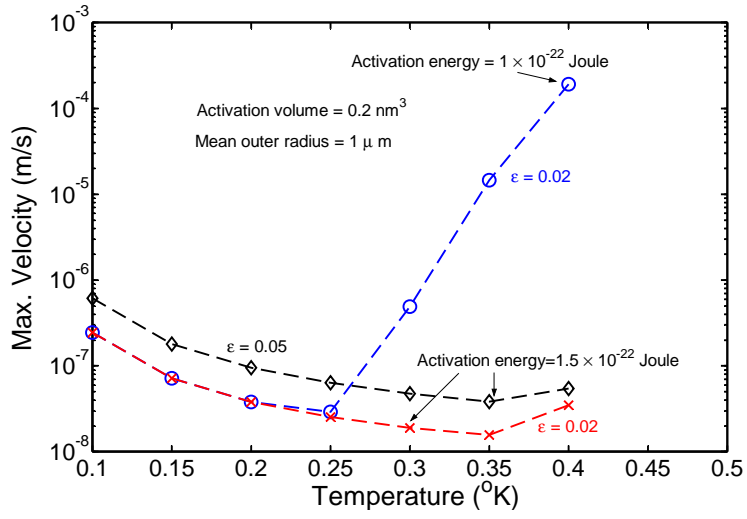


Fig. 9 Comparison of calculated (maximum) velocity (unit : m/s) using two activation energies  $1 \times 10^{-22}$  and  $1.5 \times 10^{-22}$  Joule. Around  $T \sim 0.25$  or  $0.35^\circ\text{K}$ , the monotonic trend of

velocity (or deformation rate) bifurcates as the temperature increases.

$$r_o = 1\mu\text{m and } \epsilon = 0.02, 0.05R_o.$$